16th World Conference on Earthquake, 16WCEE 2017

Santiago Chile, January 9th to 13th 2017

Paper N° 2531

Registration Code: S-V1464331694

SEISMIC ASSESSMENT FOR RETROFITTED SKEWED REINFORCED CONCRETE BRIDGES WITH BUCKLING RESTRAINED BRACES

Y. Wang[(1)], L. Ibarra[(2)], C. Pantelides[(3)]

[(1)] *Graduate Research Assistant, University of Utah, matt.wang@utah.edu*
[(2)] *Assistant Professor, University of Utah, luis.ibarra@utah.edu*
[(3)] *Professor, University of Utah, chris@civil.utah.edu*

Abstract

In this study, buckling restrained braces (BRBs) are implemented as a potential retrofit strategy to mitigate damage in skewed bridges. For this purpose, a three-span reinforced concrete (RC) box girder skewed bridge was used as a case study. A three-dimensional (3-D) model was developed in OpenSees to incorporate BRBs between bent columns. The model includes soil-structure interaction effects adjusted by recent results from skewed backfill-abutment interaction experiments. This paper assesses the impacts of five different BRB designs on the performance of skewed concrete box girder bridges with different skewed angles. Nonlinear time history analyses (THAs) were performed to assess effect of BRBs on the seismic performance of skewed bridges. The seismic behavior of skewed bridges can be significantly different from that of straight bridges due to potential torsional effects caused by the combination of longitudinal and transverse seismic responses. Therefore, optimized BRB designs were developed for a certain skew angle. The results present a considerable vulnerability of original skewed bridges to deck rotation and shear key failure. After retrofit implementation, the BRBs in column bents can redistribute and dissipate energy in transverse direction of the skewed bridges, reducing the potential failure of the abutment shear keys and concrete columns. The influence of skew angle and BRB properties were also identified.

Keywords: Skewed bridges; Buckling restrained braces; Seismic retrofit; Optimization design

1. Introduction

Many bridges located in seismic regions may suffer unrepairable damage, or even collapse when subjected to strong earthquakes. Skewed bridges are more prone to exhibit structural damage than straight bridges during seismic events. The major causes of skewed bridges failure during past earthquakes are deck unseating displacement, deck collapse due to deck in-plane rotation, shear key damage or failure, large bent drift due to bending of supporting columns, and column shear failure. Maragakis and Jennings [1] proved that the rigid body motion of the bridge deck along with the impact between the deck and the abutments can lead to severe damages on skew highway bridges. Also, Wakefield et al. [2] utilized nonlinear models to analyze seismic effects on skewed bridges, showing that their dynamic responses are dominated by in-plane rigid body motion in translation and rotation direction.

To remedy this situation, rebuilding or retrofitting of deficient bridges is necessary. The first seismically retrofitted bridge in U.S. was a Californian bridge after the 1971 San Fernando earthquake. In this retrofit, restrainer cables and high strength bars were implemented to limit the deck moment in the longitudinal direction [3]. However, the poor performance of this retrofit approach in subsequent earthquakes prompted further research on retrofit methodologies [4]. For instance, full height steel jackets were developed to enhance seismic shear capacity of RC bridge columns [5]. And composite materials such as carbon fiber reinforced polymer (CFRP) have been used to improve bridge performance at the column bents [6].

Recent studies have considered the use of buckling restrained braces (BRBs) to increase the seismic capacity of different bridge components, taking advantage of the strength and energy dissipation capabilities of these components. For example, El-Bahey and Bruneau [7] used chevron BRBs as structural fuses to dissipate seismic energy in a RC bridge bent. Also, Dusicka et al. [8] retrofitted a two-pier bent with a diagonal BRB, showing that the BRB implementation can provide for ductile response, without significant damages to the concrete elements. Upadhyay et al. [9] studied the performance of an exsiting multi-span curved bridge supported on rigidly capped vertical pile groups retrofitted with BRBs at each girder at the abutments, to prevent pouding damage. Wang et al. [10] evaluates the potential benefits of seismically rehabitlitating straight bridges by implementing BRBs between the bent columns. Analytical results proved that the BRBs in column bents can redistribute and dissipate energy in the transverse direction of the bridge, reducing the potential failure in columns, and at the abutment shear keys. This study evaluate the seismic performance of retrofit skewed bridge with different types of BRBs installed in column bents to optimize the BRB design.

2. Bridge characteristic and modeling

2.1 General description

The skew bridges selected for the study are multi-span bridges with multiple columns in each bent, and are designed in the Western U.S. The bridges are based on a three-span cast in-place RC box girder bridge with a total length of 127.5 m (425 ft), located in Ripon, CA [11]. The original bridge is expected to meet the life safety requirements without the BRB retrofit, but its operational limits may be exceeded under the design basis earthquake (DBE). The on-site bridge, as pictured in Fig. 1, has two bents and abutments skewed 36° with respect to the bridge longitudinal axis. As a baseline case, a modified straight bridge is also evaluated to separate BRB effects on bents and abutments from those caused by the bridge skewness. Each bent has three circular columns with a diameter of 1.68 m (5.6 ft), and a height of 7.38 m (24.6 ft), as shown in Fig. 2. The columns have a longitudinal reinforcement of 34 No. 14 rebars [43 mm (1.72 in) in diameter], arranged in bundles of two rebars. The columns are pin connected to the foundation, according to current design codes. As observed in Fig. 2, only the interior longitudinal reinforcement is continuously connected to the foundation, and an expansion joint filler is used around the column edges. The piers are supported on 24 HP 305 × 79 steel piles per column. The seat-type abutments have nine bearing pads and 40 piles underneath.

Fig. 1 – On-site bridge in Ripon, CA (Image captured on July 2012, Map data ©2016 Google) [12]

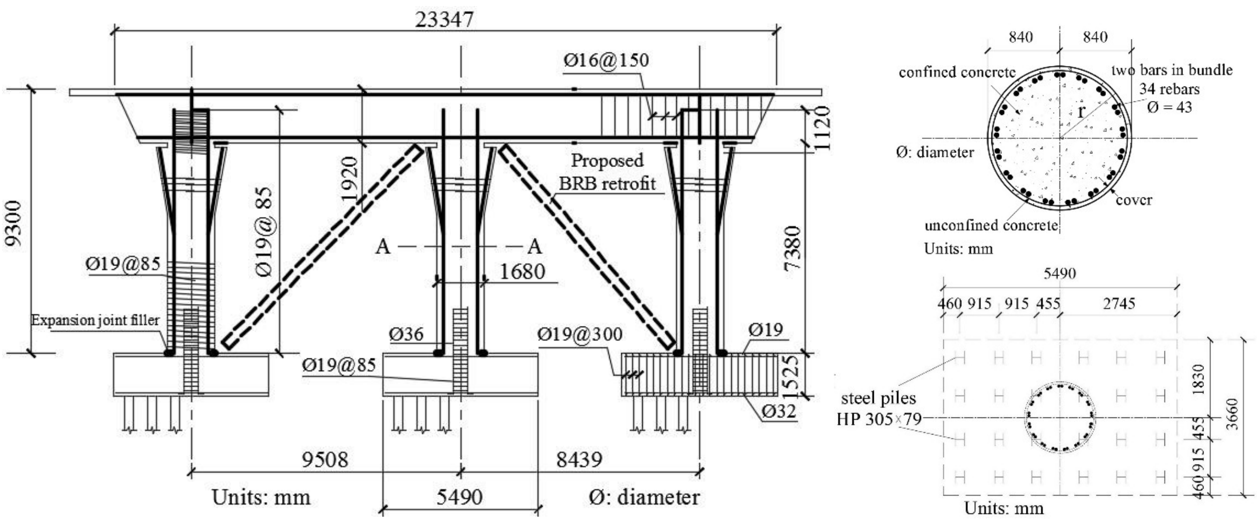

Fig. 2 – Column bent design details [10]

2.2 Bridge numerical model

The original 3-D bridge model was created in OpenSees [13] by Kaviani et al. [11]. The deck was modeled using linear-elastic beam-column elements, using the mass and moment of inertia based on the deck's net area, in agreement with Caltrans requirements. As part of this study, Kaviani's model was modified to include BRBs and a new skewed abutment system. Fig. 3 presents the retrofitted bridge with the inclusion of BRBs at the bents. The BRBs were assumed to be connected from the exterior column bottom to the top of the middle column, as shown in Figs. 2 and 3. This connection design between the steel gusset plates and the concrete components may require the implementation of steel rings around the columns, or alternatively, plates attached to the horizontal components at the face of the columns [8]. Wang et al. [10] provided a description of the "straight bridge" model and its individual components.

In previous studies [10, 11], the passive backfill response and expansion joints were represented by five nonlinear springs, and the gap elements were simulated with an OpenSees hyperbolic gap material. The longitudinal backfill stiffness, K_{abut} and strength P_{pw} are based on the recommendation from Caltrans [14]. These studies do not consider uneven longitudinal abutment responses due to the bridge skewness. Recently, however, Rollins and Jessee [15], and Marsh [16] performed several soil-structure interaction (SSI) experimental and numerical tests for skewed abutments. The results showed that the longitudinal abutment stiffness remains the same as the skew angle changes. However, the passive strength at the center of abutment decreases as the skew angle increases. Then, Marsh [16] proposed a correction factor, R_{skewed}, given by Eqn. 1, to describe the correlation between the peak passive strength of a skewed abutment ($P_{P\text{-}skew}$) and a non-skew abutment ($P_{P\text{-}no\ skew}$) as a function of skew angle θ:

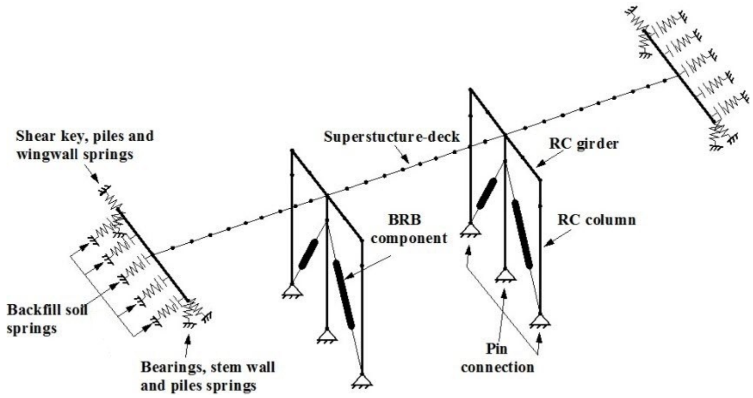

Fig. 3 – Retrofitted bridge model in OpenSees [10]

$$R_{\mathrm{skew}} = \frac{P_{P-\mathrm{skew}}}{P_{P-\mathrm{non\ skew}}} = 8.0 \times 10^{-5}\theta^2 - 0.018\theta + 1.0 \quad (1)$$

Furthermore, the different amount of backfill soil near the obtuse point (OBT) and acute point (ACU) (Fig. 3) results in a soil spring near OBT point that will have a larger stiffness and strength due to the larger soil volume behind. Considering the lack of experimental data, Kaviani et al. [11] assumed that the largest variation along the abutment is equal to 30% when the skewed angle is 60°. In this study, however, based on experimental data from Marsh [16], the definition of largest variation along the skewed abutments is adjusted to 160% when the skewed angle is 60°, as represented by Eqn. 2:

$$\bar{\beta} = 1.6 \times \frac{\tan \alpha}{\tan 60^0} \quad (2)$$

The abutment transverse stiffness includes three components: piles, shear key, and wingwalls. As recommended by Caltrans [14], the stiffness of diaphragm type abutments supported on standard piles can conservatively be estimated, ignoring the wingwalls, as 7,000 kN/m (40 kips/in) per pile. The shear key stiffness was modeled as the “strut-and-tie analogous model”, which can accurately estimate the shear key behavior, as demonstrated experimentally by Megally et al. [17]. The inclusion of the stiffness of piles and shear keys in the calculation reduced the total abutment’s stiffness, but did not change the ultimate strength of the abutment [18]. In addition, the wingwall transverse stiffness, K_{ww}, can also be estimated by modifying the longitudinal abutment stiffness using factors corresponding to wall effectiveness and participation coefficients. For the case study, the inclusion of piles, shear keys and wingwalls is considered to predict more accurate results:

$$K_{abut\_T} = \frac{K_{SK}K_{pile}}{K_{SK}+K_{pile}} + K_{ww} = 2.71\times10^5 \text{ kN/m (1,522 k/in)} \quad (3)$$

For the vertical direction, a nonlinear spring with two stiffness segments acting only in compression is implemented. The initial stiffness represents the stiffness flexibility of the elastomeric bearings and a larger second stiffness, which represents the rigid behavior of the abutment stem wall stiffness.

2.3 BRB design and modeling

The RC bent frame and the BRB form a dual system that provides lateral resistance to the bridge. Several dual systems were evaluated by modifying the BRB core area to have different BRB stiffness contributions of 25%, 40%, 50%, 60%, and 75%. In the baseline dual system, 50% of the lateral resistance capacity is assigned to the BRBs (DS-50BRB). This 50% distribution of lateral resistance results in BRB components with two core plates of 25 × 238 mm (1 × 6.25 in.) and two connection plates of 25 × 325 mm (1 × 13 in). For the detail design of all BRB components, see Wang et al. [10].

A reasonable BRB yield length ratio (core length-to-working point length ratio) $L_{core}/L = 0.55$ is used in all dual systems, whereas the BRB core area is modified to obtain different BRB stiffness. The working point is defined as the center-to-center distance. But the BRB stiffness only includes the actual design length of BRBs, without the thickness of columns. The BRB brace system could be modeled using a Two-Node Link element or Truss element. The BRB components were modeled utilizing the Menegotto-Pinto (Steel02) material in OpenSees. This model includes isotropic and kinematic hardening when including Pinching4 Material in OpenSees, and it was calibrated with experimental test results from similar BRB components.

2.4 Bridge Dynamic Characteristics

The fundamental periods of the straight bridge are T_{L1} = 0.66 s. in longitudinal direction, T_{T1} = 0.38 s. in transverse direction, and T_{V1} = 0.29 s. in vertical direction (Table 1). For the skewed bridge, the longitudinal fundamental period shortens as the transverse period elongates due to deck rotation. The BRB retrofit has a negligible effect on the longitudinal frequency of the straight bridge, but it modifies the longitudinal frequency of the skewed bridge. The first period of vibration in transverse direction has a smaller reduction in the skewed bridge due to BRB retrofit than that of the straight bridge, because part of BRB stiffness contributes to the longitudinal stiffness.

Table 1 – Bridges periods of vibration

Period of vibration	**Straight (s.)**	**Straight with BRB (s.)**	**36° Skew (s.)**	**Skew with BRB (s.)**
1st (Longitudinal dir.)	0.66	0.66	0.65	0.58
2nd (Transverse dir.)	0.38	0.28	0.40	0.32
3rd (Vertical dir.)	0.29	0.29	0.30	0.29
4th (Different dir.)	0.26	0.26	0.29	0.29

Note: The contribution percentage of BRB to lateral resistance in this table is 50% (DS-50BRB).

3. Performance limit states

As defined in the previous study [10], two concrete and steel strain performance limits are combined, as well as three limit states by consolidating the fully operational and operational limits, to evaluate the seismic performance of original and retrofit bridges.

Table 2 – Limit state definitions

Limit State	Priestley-Kowalsky Strain Limits		Drift limits
	Concrete compression strain	Steel tension strain	Vision 2000
Operational	0.004	0.01 (beam), 0.015 (column)	0.5%
Life Safety	0.018	0.06	1.5%
Near collapse	-	-	2.5%

4. Skewed bridge performance

The skewed bridge model was initially subjected to the three orthogonal accelerations of the unscaled Californian far-field ground motion 1992 Landers Earthquake (Coolwater Station). The ground motion has approximately same spectral acceleration (S_a) for the original bridge transverse fundamental period (T_{1T} = 0.40 s) and for the retrofitted bridge transverse period ($T_{1T,Rerf}$ = 0.32 s). That is, $S_a(T_{1T}) = S_a(T_{1T,Rerf})$ [10].

Fig. 4a shows that the transverse drift at the top of the bent column for the original and retrofit skewed bridge. The implemented BRBs reduces the bent drift about 35%, and lead to a seismic force redistribution between bents and abutments. For instance, the total shear skew demand in the original bridge, caused by the

Landers ground motion was 37,210 kN (8,380 kips), subdivided into 22,920 kN (5,160 kips) on the abutment components and 14,290 kN (3,220 kips) on the column bents. After the retrofit, the total shear demand decreased to 29,790 kN (6,710 kips), indicating that BRB components dissipated about 20% energy of total shear demand, but this reduction was not evenly distributed between the abutment components and column bents. The shear demand decreased in the abutment components to 13,960 kN (3,140 kips), while the shear demand of the column bents actually increased to 15,830 (3,570 kips), or about 4%. The concrete and steel strains at the top of the central column are also reduced, as shown in Figs. 4b and 4c. Also, Fig. 4d shows that abutment components are at the brink of failure in the original bridge under the evaluated seismic event. If the shear key fails, the deck translational displacement in the skew direction will not prevented, leading to unseat of the bridge deck. The performance of abutment components in retrofitted bridge, on the other hand, is almost within the linear range due to a reduction in the maximum demands of almost 60%.

However, the large bent stiffness of the retrofitted bridge leads to an increase of 50% on the column shear forces, as seen in Fig. 4c. If these shear forces are excessive, the gusset plate may be separated from the column and it could transfer the lateral forces directly to the foundation [8]. In addition, the piles shear capacity should be recomputed if the column shear demand force increases. However, according to FHWA [19], the shear pile capacity is usually not critical for steel piles placed in groups.

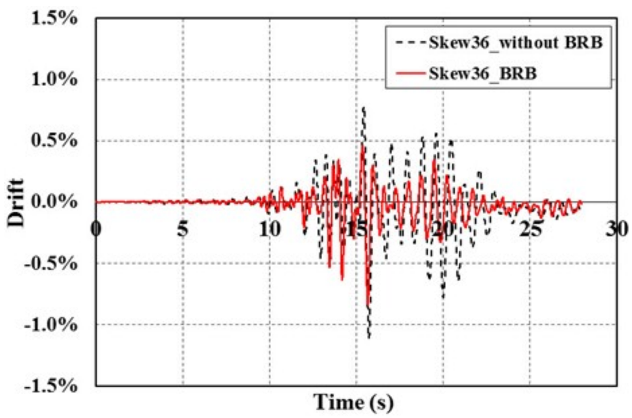

(a)

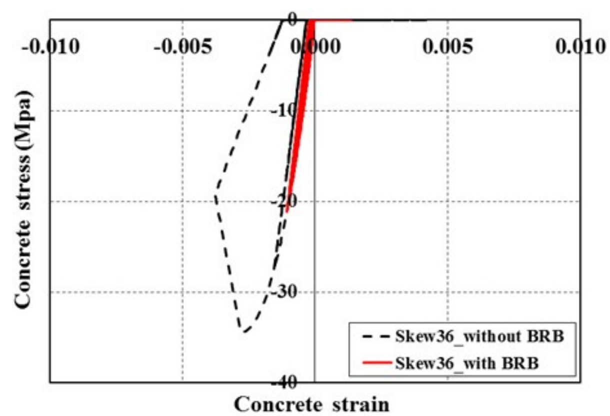

(b)

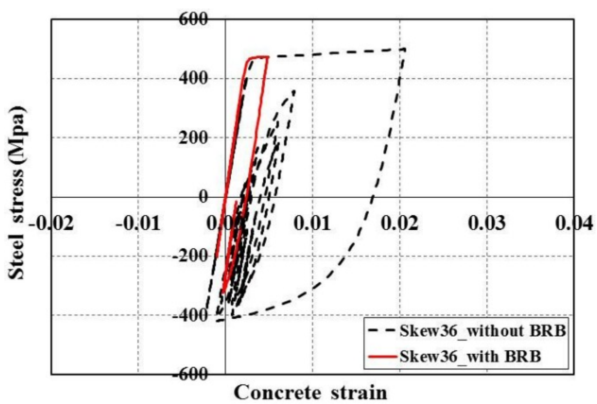

(c)

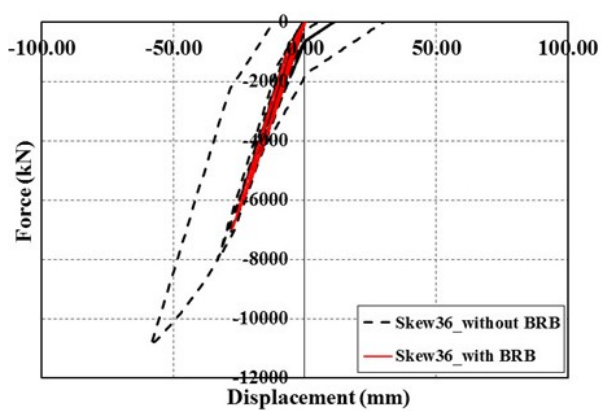

(d)

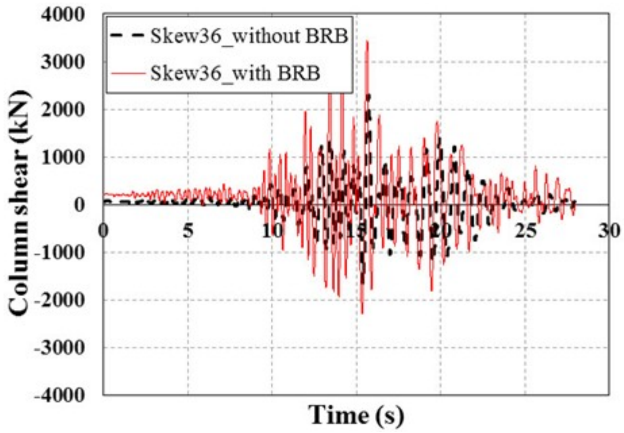

(e)

Fig. 4 – Responses of 36° skewed bridge under 1992 Landers Earthquake, 23 Coolwater Station: (a) column bent drift; (b) column concrete stress–strain; (c) column steel stress–strain; (d) abutment shear key force–displacement; (e) column shear force

5. Parametric study

A parametric study with the retrofit BRB component system was performed using 21 acceleration ground motions from the FEMA P-695 far-field record set [20].

5.1 Ground motion selection

The 21 far-field records are directly selected from FEMA P695 [20]. These records are taken from 14 events that occurred between 1971 and 1999 with magnitudes ranging from M = 6.5 to M = 7.6. Sixteen of them are classified as Site Class D (stiff soil sites), while the rest five are classified as Site Class C (very stiff soil sites), which corresponds to the studied bridge soil characteristics. Regarding site-source distance, defined as the closet distance to fault rupture, the minimum value is 11.1 km, the maximum value is 26.4 km, and the mean distance is 16.4 km.

5.2 Ground motion scaled method

In this study, a ground motion scale procedure was first used to reduce uncertainty due to record-to-record (RTR). Then, scaled paired records where applied at certain incidence angle, with respect to the longitudinal axis of skewed bridge. To reduce RTR variability, the ground motions are first rotated to minimize the correlation of covariance with major principal GMs along the transverse direction of the bridge, and minor principal GMs in the longitudinal direction. The major principal GM represents the horizontal record component with the largest spectral acceleration, $Sa(T_{T1})$, at the first period of transverse or skew direction (T_{T1} = 0.4 s.). Similar to ASCE 41-06 [21] method, each set of rotated response spectra was scaled in such a way that the average SRSS spectra in the interval $0.2T_{T1} \approx 0.1$ s. to $1.5T_{L1} \approx 1.0$ s. was equal to 1.3 times the average S_a of the MCE spectrum in this interval. In this study, $1.3S_{avg}$ = 0.933 g. As observed in Fig. 5, the dispersion of response accelerations in the target period range is greatly reduced. For instance, the logarithm standard deviation at original period (T_{T1} = 0.4 s.) was reduced from β = 0.56 to 0.38 and for the retrofit bridge with $T_{T1,Retrf}$ = 0.32 s., β was reduced from 0.54 to 0.32.

At the first stage of the study, each GM set was applied to both original straight and skewed bridges with certain incidence angle, which is defined by the angles between GM minor component input directions and the longitudinal direction of the bridges. The 0° incidence angle is defined by inputting the minor principal GM component in the longitudinal (L) direction of bridge and major principal GM in the transverse (T) direction. In the first part of the study, the GM directions are applied as shown in Fig. 6, with the GM minor component on the deck longitudinal direction (i.e.,at an angle of 0°). The effect of different incidence angles will be analyzed in the follow-up study. The retrofit base case DS50-BRB is first evaluated on both straight bridge and skewed bridge using a 0° incidence angle. Thereafter, five BRB retrofit systems are assessed on the 36° skewed bridge to optimize the BRB retrofit.

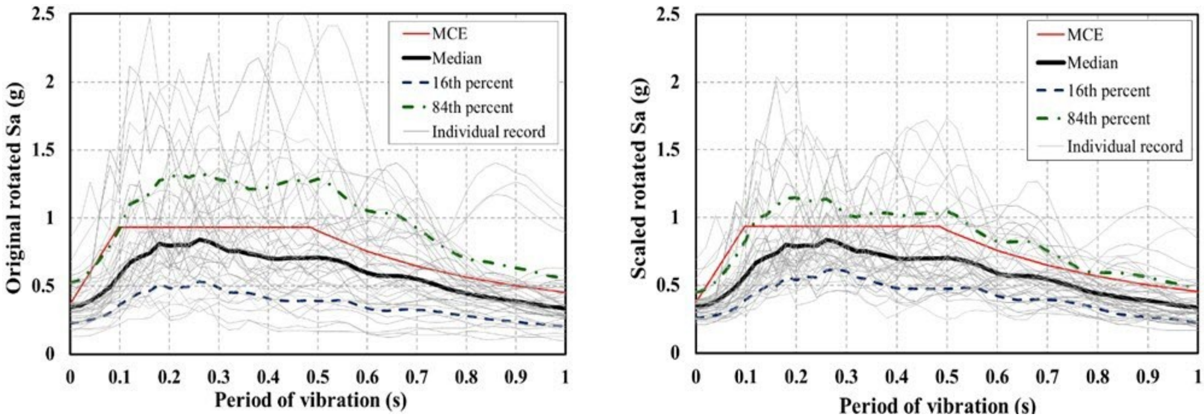

(a) (b)

Fig. 5 – Response spectrum for far-field FEMA [33] set: (a) original spectrum; (b) scaled spectrum

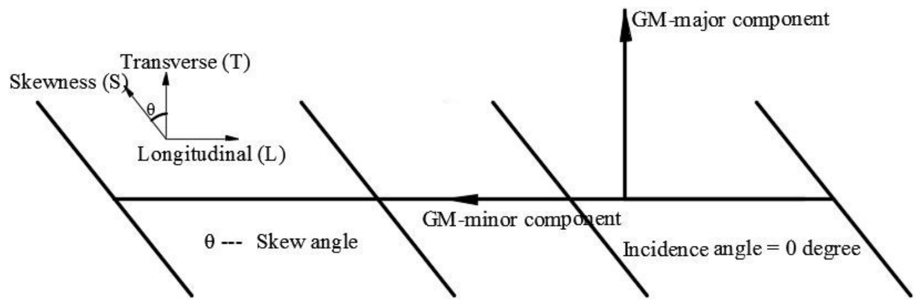

Fig. 6 – GMs set rotation direction

5.3 Results

5.3.1 BRB retrofit effects

The response of four types of bridges (original straight, retrofit straight, original 36° skewed, retrofit 36° skewed) under incidence angle of 0° (Fig. 6) are evaluated in this section. Fragility curves [or cumulative distribution functions (CDFs)] were developed for several output parameters by fitting a lognormal distribution to the data [37]. Fig. 7a shows that the total transverse demand of four types of bridges. For the case study, the original 36° skewed bridge has median seismic demands that are more than 12% larger than those of the original straight bridge. After retrofitting with BRBs, the total seismic demand is reduced about 15% for skewed and straight bridges. The dispersion in the skewed bridges are smaller than that of straight bridges because the latter always capture the combined frequency content from both horizontal GM components. The logarithm standard deviation for the response of retrofit bridges is similar to that of the original bridge design.

As can be seen in Figs. 7b and 7c, the abutment and column bent shear demands are greatly amplified by the potential rotation due to skewed configuration. The BRB retrofit reduced the abutment shear demand for both bridge types by about 30%. This confirms that BRBs can act as energy dissipation devices, preventing the typical deck unseating in skewed bridges caused by shear key failure. However, the additional stiffness provided by the BRBs redistributes seismic energy from the abutment to column bents, increasing the shear demand of the columns in both straight and skewed bridges by about 25-30%, as observed in Fig. 7c. The increase in column shear demands can be avoided by attaching the gusset plate of the BRB connection only to the foundation [8]. In the case study, however, even these increased shear column demands are still below the column shear strength.

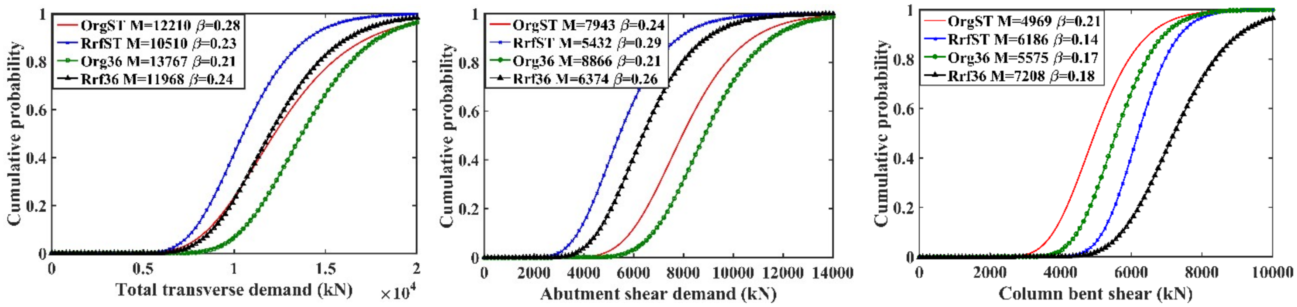

(a) (b) (c)

Fig. 7 – Cumulative distribution function of bridge shear demand: (a) Total shear demand; (b) Abutment transverse shear demand; (c) Column bent shear demand

Fig. 8a presents the fragility curves for column bent drifts of the studied bridges, as well as the operational and life safety limits. The drifts for the retrofitted straight and skewed bridges are below the life safety limit for all cases, as well as for 95% of the original straight bridge drifts. On the other hand, only 25% of the original skewed bridge drifts meet this criterion, indicating that the original 36° skewed bridge is likely to exhibit permanent damage that could lead to downtimes. Figs. 8b and 8c show the fragility curves for the concrete and steel strains at the top of the central column. In the case of steel strain, the cumulative probability under the operational limit state increases 20% for the retrofitted straight and skewed bridges. The inclusion of BRBs have larger reduction on concrete strain than that of steel strain, with more 95% retrofit concrete strain under operational limit state.

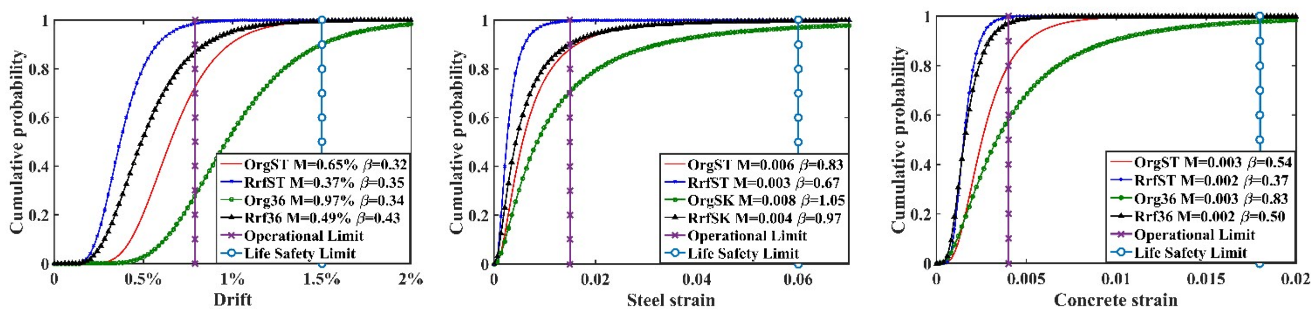

(a) (b) (c)

Fig. 8 – Cumulative distribution function of column responses: (a) Drift; (b) Steel strain; (c) Concrete strain

5.3.2 BRB core optimization in skewed bridge

The BRBs redistribute seismic energy from the abutments to the retrofitted bents, modifying the bent-to-abutment stiffness ratio, K_{bent_T}/K_{abut_T}. To evaluate these trends, skewed bridges include retrofit systems in which BRBs can withstand 25, 40, 50, 60, and 75% of the bent's shear forces (named DS-25BRB, DS-40BRB, DS-50BRB, DS-60BRB, and DS-75BRB, respectively). The hysteretic response of the five dual systems with different BRB characteristics under scaled 1992 Landers ground motions is shown in Fig. 9. As observed, the increase in the BRB core area increase the stiffness and strength of BRB dual systems. DS-75BRB system has the smallest axial drifts because of the large core plate area inhibiting BRB nonlinear behavior. Fig. 10(a) shows the total demand ratio of retrofitted 36° skewed bridge systems with respect to the original system for the five evaluated dual systems, under FEMA P-695 ground motions. The DS-60BRB has the largest demand reduction of roughly 20%, optimizing the dissipated BRB hysteretic energy. With a large core area, DS-75BRB have the same seismic demand reduction as DS-50BRB that only has half of the BRB core area [10]. Fig. 10(b) shows the abutment shear demand for the original skewed bridge and the five dual systems. As the BRB stiffness increases, the abutment shear demand decreases. However, the shear loads in the bents increase as the BRB core area [Fig. 10(c)], because the bent-to-abutment stiffness ratio becomes larger.

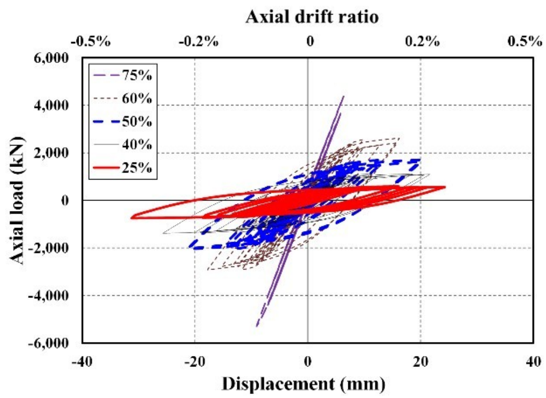

Fig. 9 –BRB hysteretic response for five dual systems under scaled 1992 Landers Earthquake, Coolwater Station

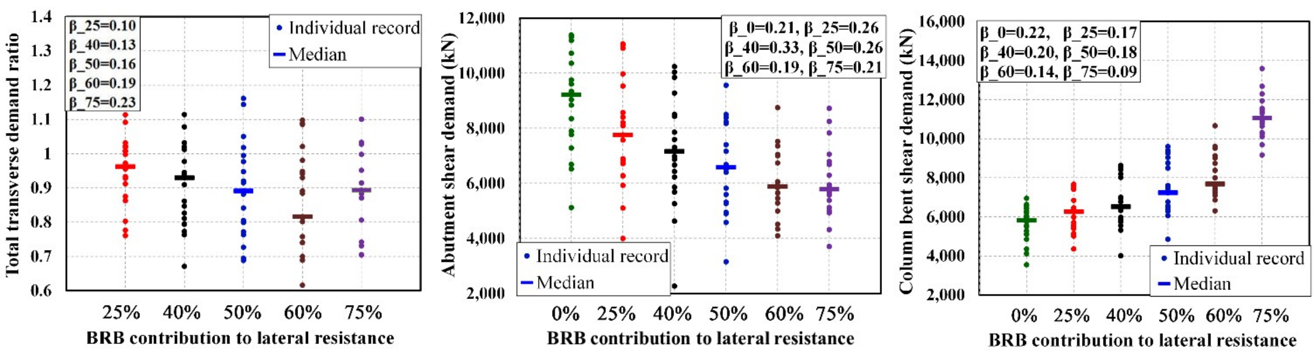

(a) (b) (c)

Fig. 10 – Comparison of different BRB designs for transverse global responses: (a) ratio of total demand of retrofitted system to total demand of original system; (b) abutment shear demand (b) column bent shear demand

Fig. 11(a) shows the bent inter-story drift ratios for the original and retrofitted 36° skewed bridges. With the additional BRB stiffness, the bent drift decreases for the retrofitted bridges. Note that the median drift ratio of the original bridge is twice as much as operational limit state, while the median drift in baseline case DS-50BRB already meets this threshold after a drift reduction of more than 50%. The BRB stiffness may greatly improve the shear demand of each column at the bent. For example, side column shear demands with DS-75BRB have all exceed the column shear strength, compromising the structural integrity of the retrofit bridge structure, as observed in Fig. 11(b). In contrast, the DS-50BRB and DS-60BRB systems have an acceptable column shear demand. As can be seen in Figs. 11(c) and 11(d), the steel tensile strain and concrete compression strain at the top of the column decreased up to 50% when the bents were retrofitted with BRBs.

6. Conclusions

The study presents a comprehensive seismic performance evaluation of skewed RC bridges retrofitted with BRBs. As structural fuses, BRBs have been implemented at the bridge bents to create a dual lateral resistance system with larger strength and stiffness. The results show that the BRBs reduce earthquake damage of skewed bridges and provide better performance by dissipating seismic energy through hysteretic behavior. The main findings of this paper are:

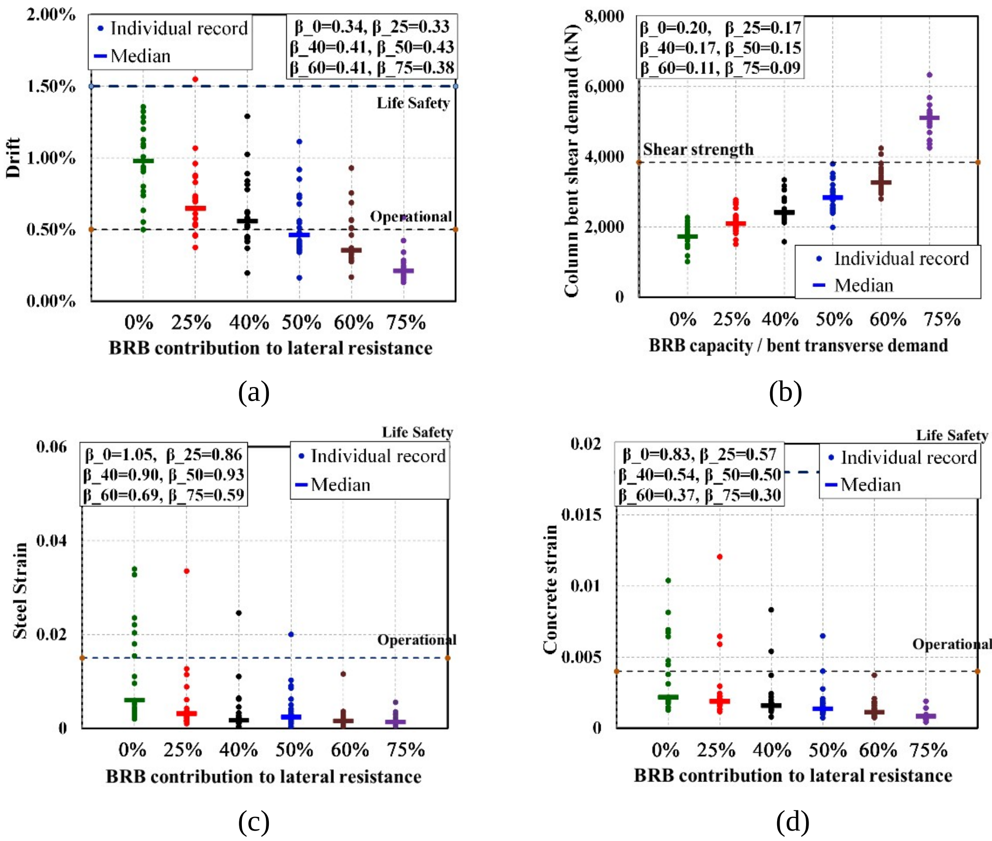

Fig. 11 – Comparison of different BRB designs for column bent responses: (a) drift; (b) side column shear; (c) steel strain; (d) steel strain

(1) The skew bridge configuration induces higher seismic demands (e.g., shear demand, bent drift, steel and concrete strain) that are from 50 to 100% larger than those of straight bridges. The additional demands compromise the structural integrity of the abutment and shear keys, and may lead to deck unseating.

(2) The implementation of BRBs reduces the bent drift up to 60% for the evaluated skew bridge, keeping the bent drift under the operational limit state. The BRBs connected to the column bents redistribute stiffness in the skew direction between column bents and abutments, and dissipate 20-25% of the bridge shear demand through BRB hysteretic behavior. The stiffness redistribution reduces the shear keys vulnerability, while increasing the bent column shear demand.

(3) The strain level of concrete and steel in columns of skewed bridges is reduced to the seismic performance of retrofit skewed by 50%.

(4) The optimal retrofit for the evaluated 36° skewed bridge was achieved by dual systems DS-50BRB (i.e., BRBs resist 50% of the elastic lateral demand) and DS-60BRB. Dual systems with larger BRBs (e.g. DS-75BRB) did not exhibit significant hysteretic energy dissipation capabilities, and may lead to column shear failure.

(5) The bridge seismic response was obtained for incidence angles rotated at intervals of 18°. For the straight bridge, the maximum response was generated when the minor principal ground motion was located along the global longitudinal direction of the skewed bridge (i.e., 0° incidence angle). For the 36° skew bridge, the maximum response was very similar for incidence angles from 0° to 36°.

6. Acknowledgements

The authors are grateful to Mountain Plains Consortium (MPC) for the financial support for this research under project MPC-421. The authors also thank Dr. Kaviani, Prof. Farzin Zareian and M. De Bortoli for providing the original bridge model in OpenSees.

8. References

[1] Maragakis, E. and Jennings, P. (1987): Analytical Models for the Rigid Body Motions of Skew Bridges. *Earthquake Engineering & Structural Dynamics*, 15(8), 923-944.

[2] Wakefield, R., Nazmy, A., Billington, D. (1991): Analysis of Seismic Failure in Skew RC Bridge. *Journal of Structure Engineering*, 117(3), 972-986.

[3] Buckle, I., Friedland, I., Mander J., Martin, G., Nutt, R. and Power, P. (2006): Seismic Retrofitting Manual for Highway Structures: part 1-bridges. *Technical Report No. FHWA-HRT-06-032*.

[4] Yashinsky, M. (1998): Performance of Bridge Seismic Retrofit during Northridge Earthquake. *Journal of Bridge Engineering*, 3(1): 1-14.

[5] Priestley, M. N., Seible, F., Xiao, Y., Verma, R. (1994): Steel Jacket Retrofitting of Reinforced Concrete Bridge Columns for Enhanced Shear Strength-part 1: Theoretical Considerations and Test Design. *ACI Structural Journal*, 91(4).

[6] Pantelides, C., Gergely, J., Reaveley, L., Volnyy, V. (1999): Retrofit of RC Bridge Pier with CFRP Advanced Composites. *Journal of Structure Engineering*, 125(10), 1094-1099.

[7] El-Bahey, S. and Bruneau, M. (2011): Buckling Restrained Braces as Structural Fuses for the Seismic Retrofit of Reinforced Concrete Bridge Bents. *Engineering Structure*, 33(3), 1052-1061.

[8] Dusicka, P., Bazaez, R., Knoles, S. (2015): Bridge Seismic Retrofit Measures Considering Subduction Zone Earthquakes. *Technical Report SPR 741*, Oregon Department of Transportation.

[9] Upadhyay, A., Pantelides, C., and Ibarra, L. (2016): Seismic performance of curved bridges on soft soils with BRB retrofit. *2016 ASCE-SEI Geotechnical and Structural Engineering Congress*, Phoenix, AZ.

[10] Wang, Y., Ibarra, L., Pantelides, C. (2016): Seismic Retrofit of a Three-Span RC Bridge with Buckling-Restrained Braces. *Journal of Bridge Engineering*, 04016073-12.

[11] Kaviani, P., Zareian, F., Taciroglu, E. (2012): Seismic Behavior of Reinforced Concrete Bridges with Skew-angled Seat-type Abutments. *Engineering Structure*, 45, 137-150.

[12] Google Map. (2016): Google street view of Ripon, CA, https://www.google.com/maps/place/Ripon,+CA+95366.

[13] McKenna, F. (2014): Open System for Earthquake Engineering Simulation, UC, Berkeley.

[14] Caltrans (2013): Seismic Design Criteria version 1.7, *California Department of Transportation*, Sacramento, California.

[15] Rollins, K. and Jessee, S. (2012): Passive Force-Deflection Curves for Skewed Abutments, *Journal of Bridge Engineering*, 18(10).

[16] Marsh, A. (2013): Evaluation of Passive Force on Skewed Bridge Abutments with Large-Scale Tests, *Ph.D dissertation*, Brigham Young University, Provo, UT.

[17] Megally, S., Silva, P., Seible, F. (2002): Seismic Response of Sacrificial Shear Keys in Bridge Abutments, *Technical Report No. SSRP-2001/23*. UC San Diego, CA.

[18] Goel, R., and Chopra, A. (2008): Role of shear keys in seismic behavior of bridges crossing fault-rupture zones, *Journal of Bridge Engineering*, 13(4), 398-408.

[19] FHWA (Federal Highway Administration). (2003): LRFD Design Example for Steel Girder Superstructure Bridge. *Technical Report FHWA NHI-04-041*.

[20] FEMA (2009): Quantification of Building Seismic Performance Factors, *Technical Report FEMA P695*, Federal Emergency Management Agency.

[21] ASCE. (2006): *Seismic Rehabilitation of Existing Buildings*, 41-13, Reston, VA

[22] Ibarra, L. and Krawinkler, H. (2005): Global Collapse of Frame Structures under Seismic Excitations, *Technical Report PEER 2015/06*, Pacific Earthquake Engineering Research Center.